Atmos. Meas. Tech., 5, 2143–2160, 2012
www.atmos-meas-tech.net/5/2143/2012/
doi:10.5194/amt-5-2143-2012

Atmospheric Measurement Techniques

Evaluating nighttime CALIOP 0.532 μm aerosol optical depth and extinction coefficient retrievals

J. R. Campbell[1], J. L. Tackett[2], J. S. Reid[1], J. Zhang[3], C. A. Curtis[1], E. J. Hyer[1], W. R. Sessions[4], D. L. Westphal[1], J. M. Prospero[5], E. J. Welton[6], A. H. Omar[7], M. A. Vaughan[7], and D. M. Winker[7]

[1]Aerosol and Radiation Sciences Section, Marine Meteorology Division, Naval Research Laboratory, Monterey, CA, USA
[2]Science Systems Applications Inc., c/o NASA Langley Research Center, Hampton Roads, VA, USA
[3]Department of Atmospheric Science, University of North Dakota, Grand Folks, ND, USA
[4]Computer Sciences Corporation, c/o Aerosol and Radiation Sciences Section, Marine Meteorology Division, Naval Research Laboratory, Monterey, CA, USA
[5]Rosenstiel School of Marine and Atmospheric Science, University of Miami, Miami, FL, USA
[6]NASA Goddard Space Flight Center, Greenbelt, MD, USA
[7]NASA Langley Research Center, Hampton Roads, VA, USA

Correspondence to: J. R. Campbell (james.campbell@nrlmry.navy.mil)

Received: 16 February 2012 – Published in Atmos. Meas. Tech. Discuss.: 11 April 2012
Revised: 26 July 2012 – Accepted: 31 July 2012 – Published: 5 September 2012

Abstract. NASA Cloud Aerosol Lidar with Orthogonal Polarization (CALIOP) Version 3.01 5-km nighttime 0.532 μm aerosol optical depth (AOD) datasets from 2007 are screened, averaged and evaluated at 1° × 1° resolution versus corresponding/co-incident 0.550 μm AOD derived using the *US Navy Aerosol Analysis and Prediction System* (NAAPS), featuring two-dimensional variational assimilation of quality-assured NASA Moderate Resolution Imaging Spectroradiometer (MODIS) and Multi-angle Imaging Spectroradiometer (MISR) AOD. In the absence of sunlight, since passive radiometric AOD retrievals rely overwhelmingly on scattered radiances, the model represents one of the few practical global estimates available from which to attempt such a validation. Daytime comparisons, though, provide useful context. Regional-mean CALIOP vertical profiles of night/day 0.532 μm extinction coefficient are compared with 0.523/0.532 μm ground-based lidar measurements to investigate representativeness and diurnal variability. In this analysis, mean nighttime CALIOP AOD are mostly lower than daytime (0.121 vs. 0.126 for all aggregated data points, and 0.099 vs. 0.102 when averaged globally per normalised 1° × 1° bin), though the relationship is reversed over land and coastal regions when the data are averaged per normalised bin (0.134/0.108 vs. 0140/0.112, respectively). Offsets assessed within single bins alone approach ±20 %. CALIOP AOD, both day and night, are higher than NAAPS over land (0.137 vs. 0.124) and equal over water (0.082 vs. 0.083) when averaged globally per normalised bin. However, for all data points inclusive, NAAPS exceeds CALIOP over land, coast and ocean, both day and night. Again, differences assessed within single bins approach 50 % in extreme cases. Correlation between CALIOP and NAAPS AOD is comparable during both day and night. Higher correlation is found nearest the equator, both as a function of sample size and relative signal magnitudes inherent at these latitudes. Root mean square deviation between CALIOP and NAAPS varies between 0.1 and 0.3 globally during both day/night. Averaging of CALIOP along-track AOD data points within a single NAAPS grid bin improves correlation and RMSD, though day/night and land/ocean biases persist and are believed systematic. Vertical profiles of extinction coefficient derived in the Caribbean compare well with ground-based lidar observations, though potentially anomalous selection of a priori lidar ratios for CALIOP retrievals is likely inducing some discrepancies. Mean effective aerosol layer top heights are stable between day and night, indicating consistent layer-identification diurnally, which is noteworthy considering the potential limiting effects of ambient solar noise during day.

Published by Copernicus Publications on behalf of the European Geosciences Union.

1 Introduction

Launched into orbit in 2006, the three-channel Cloud Aerosol Lidar with Orthogonal Polarization instrument (0.532 μm with linear polarization diversity, and 1.064 μm; CALIOP) flown aboard the National Aeronautics and Space Administration (NASA) and Centre National d'Études Spatiales (CNES) Cloud-Aerosol Lidar and Infrared Pathfinder Satellite Observation (CALIPSO) satellite has collected the first global, inter-seasonal and multi-annual profiles of aerosol particle and optically thin cloud structure from space (Winker et al., 2009, 2010). The vertical profile for aerosol particle electro-optical scattering, in particular, is a unique and highly synergistic satellite measurement, since passive aerosol-focused remote sensors alone are limited at best in observing vertically resolved information with reasonably high resolution. CALIOP profiling has, thus, benefitted a number of aerosol research initiatives, including global particle transport studies (e.g., Uno et al., 2009), surface emission estimates and injection scenario characterisation (e.g., Bessagnet et al., 2008; Amiridis et al., 2010), pyrocumulonimbus plume identification and dispersion (Fromm et al., 2010), volcanic plume monitoring (e.g., Carn et al., 2009; Campbell et al., 2012a), coupled two/three-dimensional variational (2D/3DVAR) data assimilation for global mass transport forecasting (e.g., Campbell et al., 2010; Zhang et al., 2011), four-dimensional ensemble Kalman filter data assimilation (e.g., Sekiyama et al., 2010), and transport model validation (e.g., Uno et al., 2008; Yumimoto et al., 2008).

Calibration of CALIOP signals (e.g., Powell et al., 2009; Rogers et al., 2011) and verification/validation of value-added (i.e., Level 2.0 and higher) NASA data products (e.g., Liu et al., 2009; Kacenelenbogen et al., 2011) ensure that high-accuracy data are available for researchers and that the archive is consistent for legacy study long after the mission is completed. Kittaka et al. (2011) recently compare 0.532 μm aerosol optical depth (AOD) retrievals reported in the NASA Version 2.01 CALIOP 5-km Aerosol Layer product versus 0.550 μm AOD retrievals based on measurements made by the NASA Moderate Resolution Imaging Spectroradiometer (MODIS) aboard the Aqua satellite and, thus, collected in formation and approximately 5 min before CALIOP as part of the NASA "A-Train" constellation (e.g., Stephens et al., 2002). Naturally, this work relates only to half of all available CALIOP AOD data, since MODIS retrievals are based on scattered solar radiances. Given that the lidar is duly capable of nighttime measurements, additional validation is necessary to fully evaluate CALIOP aerosol retrieval performance. Furthermore, given that particle layer identification and the accuracy of the CALIOP-derived 0.532 μm extinction coefficient and, thus, its column-integrated sum AOD, are each a function of the amount of ambient solar background light measured in any given scattering profile (i.e., noise; Hunt et al., 2009; Liu et al., 2009; Vaughan et al., 2009; Young and Vaughan, 2009), nighttime AOD retrievals should exhibit relative accuracies and skill that differ from, and nominally exceed, those from daytime.

Therefore, in this paper, quality-assured (QA) Version 3.01 CALIOP Level 2 5-km 0.532 μm nighttime AOD are evaluated from 2007 at $1° \times 1°$ resolution versus an aerosol forecast model equipped with a 2DVAR (x, y) assimilation scheme for QA AOD datasets from Terra and Aqua MODIS and the NASA Multi-angle Imaging Spectroradiometer (MISR). The study includes all 2007 QA CALIOP 5-km aerosol profiles available where column-integrated AOD $\neq 0$, no cloud was present within the along-track average and an aerosol particle layer was resolved to within 250 m of the surface, thus, limiting undersampling and sample bias caused by transmission loss and/or scattering ambiguities through the profile. The *US Navy Aerosol Analysis and Prediction System* (NAAPS) is a $1° \times 1°$ global aerosol mass transport model used for computing 6-day forecasts of smoke, dust, sulfate, sea salt and SO_2 mass concentration every 6 h. Global and regional mean CALIOP AOD, correlation coefficients and root-mean-square deviation are derived relative to corresponding 0.550 μm NAAPS AOD to qualitatively assess day/night retrieval skill and accuracies and quantitatively estimate relative offsets. Profiles of CALIOP-derived 0.532 μm extinction coefficient are further compared versus ground-based lidar measurements to investigate representativeness, potential bias and identify any diurnal variability present. The goal of this work is to motivate a practical study of CALIOP nighttime aerosol algorithm performance using one of the few estimates of AOD available globally during darkness.

2 CALIOP/NAAPS AOD datasets and model skill versus MODIS and AERONET

2.1 2007 CALIOP and NAAPS AOD datasets

The Version 3.01 CALIOP Level 2 Aerosol Profile product (L2-AProf) includes 0.532 μm extinction coefficient profiles with corresponding retrieval uncertainties derived in 5-km along-track segments at 60 m vertical resolution, separated into contiguous daytime and nighttime granule files. As CALIOP is an elastic-backscatter lidar instrument, the extinction coefficient is derived using the Hybrid Extinction Retrieval Algorithm (HERA; Young and Vaughan, 2009), based on a priori selection of a multiple-scattering correction factor (nominally set to unity for aerosols) and the ratio for extinction and backscatter coefficients. The latter term, the so-called "lidar ratio", is assumed constant vertically within detected layers (Omar et al., 2009) and is used for solving the single elastic-scattering lidar equation that contains these two separate and unknown quantities (Young and Vaughan, 2009; Oo and Holz, 2011). Retrieval uncertainties begin with an estimate of the signal noise scale factor, and are computed at each range bin reported in the Level 1B attenuated

backscatter product at 20.16 Hz pulse repetition frequency and 30/60 m vertical resolutions, for 0.0 to 8.2 and 8.2 to 20.1 km above mean sea level (m.s.l.), respectively (Liu et al., 2006). Since the CALIPSO 98.2° retrograde satellite orbit limits the poleward extent of the polar-orbiting ground track, only data between 80° N/S are analysed (referred to as "global" for simplicity).

The 2007 dataset was chosen for this analysis for its lack of significant data gaps and singular use of the primary instrument laser system throughout that year (Hunt et al., 2009). To ensure that only QA measurements are included, each L2-AProf 5-km extinction profile solved was screened and low-confidence data points excluded before integrating and solving column AOD. Within each data file disseminated by NASA, parameter profiles are included reflecting various diagnostic quality flags for the user to consider for QA evaluation. These terms are defined and described elsewhere (NASA, 2010). Specifically then for a given 5-km profile, an extinction coefficient value is considered QA and included in the column-integrated sum (i.e., AOD), when at the corresponding range either

1. Extinction_QC_532 (r) is equal to 0, 1, 2, 16 or 18,
2. $-20 \geq$ CAD_Score (r) ≥ -100,
3. Extinction_Coefficient_Uncertainty_532 (r) $\leq 10\,\mathrm{km}^{-1}$,
4. Atmospheric_Volume_Description ($r*$, bits 1–3) is equal to 3, or
5. Atmospheric_Volume_Description ($r*$, bits 10–12) is not equal to 0,

where (r) relates each value as a function of range.

Extinction_QC_532 reports on the type of retrieval used for solving extinction (constrained versus unconstrained), whether or not the subject layer was opaque and the result of the process (convergent, divergent or oscillating). Should the initial lidar ratio chosen deviate significantly from reality, the solution diverges. The algorithm then adjusts the a priori value in order to reiterate and reevaluate. If a stable result is not derived, and/or if the solution does not fall within a range of acceptable values for AOD and/or magnitudes of extinction coefficient, the Extinction_QC_532 (r) parameter setting reflects the instability. CAD_Score reflects confidence of the classification of a layer as aerosol or cloud within a bin. Extinction_Coefficient_Uncertainty values exceeding $10\,\mathrm{km}^{-1}$ reflect increasingly unrepresentative values, though this setting is conservative, as the parameter is set to $99\,\mathrm{km}^{-1}$ for retrievals deemed unstable. Atmospheric_Volume_Description at bits 1–3 describes the type of scattering target identified, where a value of "3" indicates aerosol particle presence. Bits 10–12 denote the type of aerosol particle identified. Here, "0" represents "not determined" cases, which are rejected. Aerosol particle extinction profiles that contain only fill values after screening (i.e., AOD = 0) indicate regions of the atmosphere where the mass loading lies below the instrument detection limits. These profiles are removed from the sub-sample.

Winker et al. (2012) describe a similar rubric for filtering L2-AProf retrievals and achieving what they designate as Level 3 QA status. They further discuss the ramifications of tuning each metric. The study here is, thus, unique to this five-step screening process, though differences from that used by Winker et al. (2012) are considered slight. For example, they reject values for Extinction_QC_532 (r) set equal to 2 (unitless), and only reject values for Extinction_Coefficient_Uncertainty_532 (r) equal to $99\,\mathrm{km}^{-1}$. Cases of Extinction_QC_532 (r) equal to 2 represent less than 2 % of all 2010 nighttime data, for example. Other screening metrics are used that remove misclassified cirrus clouds, aerosol layers attributable to noise and surface contamination. The consequences of these latter steps are believed mostly negligible for their impact on mean AOD values studied here, though future work is necessary to ensure this.

Since L2-AProf includes data reported at 60 m vertical resolution, measurements below 8.2 km m.s.l. reflect two-bin averages of raw 30 m resolution data. Consecutive 30 m bins reflecting either cloud or aerosol scattering are never averaged together to yield a single 60 m bin in the L2-AProf file. Therefore, with (4) and (5), $r*$ relates to the possibility that one of the two bins used for creating the average value may not correspond with an Atmospheric_Volume_Description value equal to 3, though the other must. Since such a bin cannot represent cloud, and must instead be either "Clear Air", or "Surface Return", and the extinction coefficient is not reported for these bin types, we include these 60 m data points in the analysis, for they reflect the corresponding aerosol-related value specifically. Only those bins between the surface and 10.0 km above mean sea level (m.s.l.) are analysed.

Two additional screening metrics are applied to the sample. First, profiles where cloud was present at any range (Atmospheric_Volume_Description equal to 2) within the 5-km along-track average are removed. Cloud scattering can negatively influence the aerosol particle scattering profile and subsequent retrievals of corresponding extinction and backscatter coefficients, since transmission losses must be corrected for when aerosol layers are below any transmissive cloud base. In this latter scenario, and/or when clouds are embedded within aerosol particle layers, full source pulse attenuation for most lidar instruments occurs at visible optical depths approaching 3.0 (Sassen and Cho, 1992). Accordingly, as a second screening metric, profiles are removed if aerosol particle scattering is not detected to within 250 m of the surface in the 5-km along-track average. Like clouds, dense aerosol layers can exhibit visible optical depths approaching 3.0, thus, limiting CALIOP profiling to the surface (Hunt et al., 2009; Vaughan et al., 2009; Liu et al., 2011). This metric screens profiles limited by simple undersampling, in addition to cases where optically-thin aerosol

particle layers scatter at magnitudes below layer-detection thresholds.

Each QA 5-km CALIOP L2-AProf profile and AOD data point is sorted into a global $1^\circ \times 1^\circ$ grid matching the NAAPS model domain based on the centre of the 5-km along-track data average. The data are then paired with the corresponding 0.550 μm AOD retrieved from the closest six-hourly NAAPS 00-h model analysis derived after assimilation. 2DVAR NAAPS assimilation is conducted using the Navy Atmospheric Variational Data Assimilation System (NAVDAS) for Aerosol Optical Depth (NAVDAS-AOD; Zhang et al., 2005; Zhang and Reid, 2006, 2009). QA MODIS over-ocean (Zhang and Reid, 2006; Shi et al., 2011a) and over-land AOD (Hyer et al., 2011) products and Version 1 of an assimilation-grade MISR AOD product (Shi, 2009) are system inputs. Descriptions of NAVDAS-AOD and its impact on NAAPS performance are given by Zhang et al. (2008) and Reid et al. (2009). Global AOD derived with NAAPS after 2DVAR MODIS and MISR assimilation are validated using quality-assured Level 2 NASA Aerosol Robotic Network measurements (AERONET; Holben et al., 1998). With 2DVAR assimilation, the model exhibits accuracies comparable to that of satellite retrievals (e.g., Zhang et al., 2008; Zhang and Reid, 2010; Hyer et al., 2011), and forecasts are improved by 20–40 % (Zhang et al., 2008, 2011; Zhang and Reid, 2010).

Given that NAAPS assimilates MODIS and MISR AOD, model errors co-vary closely with those inherent to the satellite datasets (discussed/introduced below, and as will be depicted in Figs. 1c and 2c). Skill, uncertainty and retrieval bias for both MODIS and MISR AOD have been evaluated and reported (e.g., Hsu et al., 2004; Martonchik et al., 2004; Remer et al., 2005; Redemann et al., 2006; Zhang and Reid, 2006; Kahn et al., 2007, 2009; Hyer et al., 2011; Shi et al., 2011a, b). NAAPS exhibits similar tendencies (e.g., Zhang and Reid, 2009). However, QA screening limits error propagation into the model. For example, empirical corrections compensate for MODIS retrievals involving dust particles, which can be high by as much as 10–20 %, and for fine-mode fractional AOD that can be low by a similar amount (Hyer et al., 2011). Though MISR biases are relatively less intrusive (Shi et al., 2011b), the instrument operates with a relatively limited viewing swath compared with MODIS and global coverage is achieved only once every eight days (e.g., Diner et al., 2002).

2.2 NAAPS Skill versus MODIS/MISR and AERONET

NAAPS AOD analyses reflect the influence of the free-running model forecast, as well as AOD assimilation (i.e., MODIS and MISR) in sunlit sectors at 00-h. NAAPS AOD in the nighttime (i.e., dark) sector at 00-h, used here, thus, reflect the influence of at least 12 h of model integration since AOD was last assimilated. Zhang et al. (2011) report mean global 0.550 μm AOD error at 12-h relative to AERONET near 0.075. However, this considers only the sunlit sector of the model at 12-h, where validation data are available, but with no assimilation having occurred at initialisation. NAAPS skill within the dark sector of the forecast at 12-h is undetermined. Therefore, uncertainties of the NAAPS 0.550 μm AOD considered here must be inferred from interpolating between the two surrounding time steps, 00 and 24-h. The magnitude of the global mean error is very likely less than ~ 0.075, though, given potential assimilation within the sunlit sector at model initialisation, in contrast to Zhang et al. (2011).

Shown in Fig. 1 are mean NAAPS 00-h analysis and co-incident integrated 0.550 μm QA MODIS and 0.557 μm MISR AOD during 2007, correlation coefficient and root-mean-square-deviation (RMSD) between the two, number of data points and the ratio of NAAPS to MODIS/MISR AOD (differences between MODIS and MISR wavelengths are presumed negligible, given the relative uncertainty necessary for interpolating MISR to 0.550 μm). NAAPS resolves areas of persistently high AOD well compared with MODIS/MISR (Fig. 1a and b). Globally, correlation coefficients exceed 0.8 (Fig. 1c) and RMSD ranges between 0.02–0.10 (Fig. 1d), though select regions peak over 0.20 (east-central Asia, being most notable). Relative AOD ratios between the two are near unity (Fig. 1f). Some bias is present, predominantly over land, where fewer suitable satellite retrievals are available (e.g., Hyer et al., 2011) and model source functions exert stronger influence. For instance, NAAPS is relatively high over Sahara, southern Africa and western Australia, and low over the western United States and east-central Asia. Again, as described above, the consistency depicted in these results is a direct response of the model to its assimilation inputs.

Corresponding findings for the 24-h NAAPS forecast are shown in Fig. 2. Skill degradation is apparent. The model retains most of the regional structure depicted in the MODIS/MISR composite (Fig. 2a versus b). However, correlation drops, with only a few regions maintaining a value above 0.8 (Fig. 2c). RMSD increases (Fig. 2d) over corresponding high-biased regions, which are greatly enhanced, over western Sahara, central and southern Africa, and eastern/south-central Asia (Fig. 2f). As a whole, the model is biased slightly high globally, on average, nearing 20 % compared with the satellites. This is somewhat deceptive, however, since many of these regions, including the oceans, typically exhibit relatively low mean AOD on the order of 0.10 or lower at 0.550 μm, such that a 10 % offset (0.01) can create relatively large apparent differences.

When evaluating 2007 NAAPS AOD with coincident AERONET ground-based observations, many of the interpretations of Figs. 1 and 2 are reinforced (Fig. 3). For the 00-h model analysis, AOD correlation varies from 0.82 to 0.83 at over-land and coastal sites, respectively, with absolute errors from 0.063 to 0.077. For the 24-h forecast, AOD correlation drops to 0.69 and 0.77, respectively, and absolute

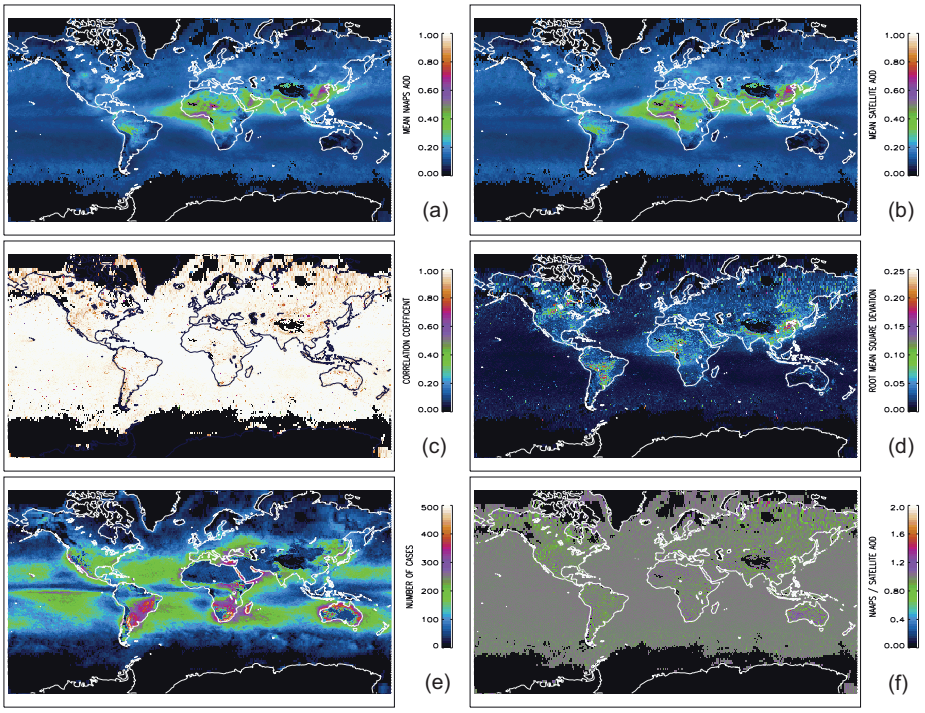

Fig. 1. For 2007 at 1° × 1° global resolution, **(a)** mean 0.550 µm NAAPS 00-h analysis aerosol optical depth (AOD) for data points with co-incident 0.550 µm MODIS and/or 0.557 µm MISR AOD retrieval (i.e., daytime), **(b)** corresponding MODIS/MISR mean AOD, **(c)** correlation coefficient between the two datasets for all points inclusive, **(d)** root-mean-square deviation between the two, **(e)** number of cases per grid bin and **(f)** the corresponding ratio of mean NAAPS to MODIS/MISR AOD.

error rises accordingly to 0.077 and 0.092. These results are similar to those recently reported by Zhang et al. (2011).

In summary, whereas a comprehensive quantitative assessment of CALIOP AOD retrievals based on NAAPS is undeterminable, interpretation of the differences between day/night performance and, thus, the identification of potential bias, are qualitatively feasible. Each dataset exhibits characteristic uncertainties that exceed even the slight offset expected between the two due to the difference in wavelength (3 % for an Angstrom Exponent of 1.0). However, since CALIOP AOD retrievals are algorithm/retrieval dependent (i.e., not direct measurements), it is relevant that the nighttime global database be investigated and compared with those for daytime in a relative sense in order to underscore performance strengths and/or identify issues requiring technical improvements. Both steps will lead to a more consolidated mission archive, advancing our understanding of global elastic-scattering lidar instrument observations and providing a logical framework for future projects. The results depicted in Figs. 1–3 indicate that nighttime NAAPS AOD represent a stable estimate of AOD for this purpose.

3 CALIOP AOD retrievals versus NAAPS: nighttime and daytime assessment

3.1 Global Aerosol Optical Depths

This section begins with an assessment of mean day/night 2007 CALIOP QA 0.532 µm AOD derived at 1° × 1° global resolution, comparing with NAAPS as a reference dataset. Not every 1° × 1° grid bin contains CALIOP data. This is a result of the CALIPSO polar-orbiting ground track and causes striping of null data points in the global composite images shown. Anderson et al. (2003) show that the horizontal covariance of aerosol physical properties exhibits a mean e-folding distance of only a few hundred kilometres, which was subsequently verified solely from satellite observations by Zhang et al. (2008). Since a CALIOP QA observation is assigned to the closest NAAPS grid bin based on the centre of its 5-km along-track data average, which can result in a nearly 80 km offset at the equator, the bulk of the points making up each bin average will fall within a range where autocorrelation nominally exceeds 0.8.

Shown in Table 1 are mean AOD for both day, night, day/night ratio and total from the 2007 QA CALIOP and corresponding NAAPS sub-sample, derived both for all data points inclusive and where each 1° × 1° bin mean value is treated as a single normalised point in spite of

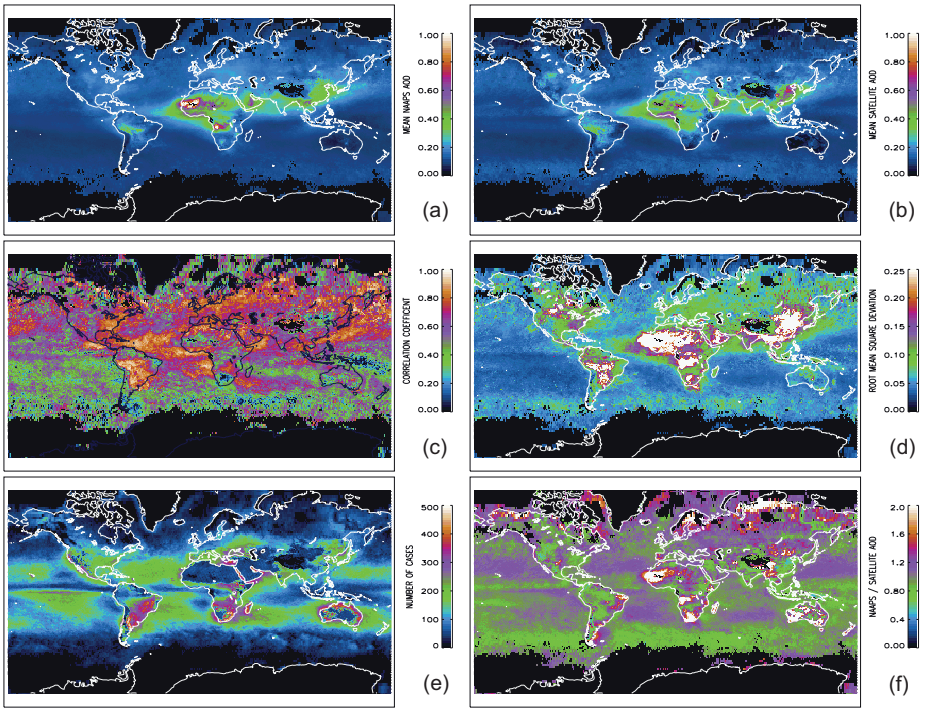

Fig. 2. For 2007 at 1° × 1° global resolution, **(a)** mean NAAPS 24-h forecast AOD for data points with co-incident 0.550 µm MODIS and/or 0.557 µm MISR AOD retrieval (i.e., daytime), **(b)** corresponding MODIS/MISR mean AOD, **(c)** correlation coefficient between the two datasets for all points inclusive, **(d)** root-mean-square deviation between the two, **(e)** number of cases per grid bin and **(f)** the corresponding ratio of mean NAAPS to MODIS/MISR AOD.

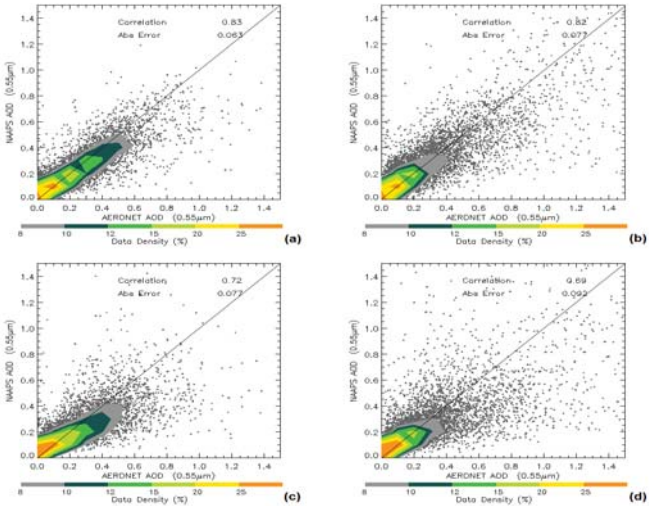

Fig. 3. For 2007, comparisons of NAAPS and co-incident AERONET 0.550 µm AOD measurements for the 00-h model analysis at **(a)** over-ocean and **(b)** over-land sites, and the 24-h forecast model analysis at **(c)** over-ocean and **(d)** over-land sites. Corresponding correlation and absolute error for each profile are given in the inset. One-to-one ratio lines are superimposed.

any offsets in relative sample size globally. The analysis is broken out relative to the surface type attributed to the NAAPS model domain (over-land, coast and ocean). For all data points, global mean CALIOP AOD is 0.126 during day, 0.121 at night (+4.4 % day/night offset) and 0.123 total, compared with NAAPS at 0.132, 0.136 (−2.8 % day/night offset) and 0.134, respectively. When normalised per bin, thus, compensating for differences in sample size within the aggregate mean, CALIOP values are 0.102, 0.099 (+2.5 % day/night offset) and 0.101, compared with 0.097, 0.097 (0.0 % day/night offset) and 0.097 from NAAPS. Note that over-ocean mean CALIOP and NAAPS AOD in both scenarios from Table 1 is at least 10 % lower than the 0.120 0.550 µm AOD global mean approximated from Zhang and Reid (2010) and their 2007 QA MODIS dataset. This likely reflects more accurate cloud screening available from CALIOP relative to the passive datasets assimilated by NAAPS, and the offset may approximate a lingering passive AOD bias present in these carefully-screened datasets due to optically-thin clouds. This finding requires further study and analysis.

Mean nighttime 2007 QA CALIOP AOD are shown at 1° × 1° resolution in Fig. 4a, depicting the prominent aerosol features found in the corresponding NAAPS composite (Fig. 4b). Correlation between the two datasets (Fig. 4c) ranges mostly between 0.30 and 0.70 per bin, increasing near

Table 1. For the QA 2007 CALIOP and corresponding NAAPS sub-sample, mean AOD over-land, coastal and ocean regions for day, night, day/night ratio, total and sample sizes, calculated both for all points inclusive and in a weighted format per 1° ×1° NAAPS grid bin.

		Land		Coast		Ocean		Total	
		CALIOP	NAAPS	CALIOP	NAAPS	CALIOP	NAAPS	CALIOP	NAAPS
All data	Day	0.219	0.231	0.148	0.161	0.102	0.107	0.126	0.132
	Night	0.204	0.231	0.154	0.158	0.090	0.102	0.121	0.136
	Ratio	1.075	1.001	0.959	1.018	1.134	1.046	1.044	0.972
	Total	0.210	0.231	0.151	0.159	0.096	0.104	0.123	0.134
	Sample	Day: 465 530 (19 %) Night: 685 098 (25 %)		Day: 100 569 (4 %) Night: 121 057 (4 %)		Day: 1 905 766 (77 %) Night: 1 985 218 (71 %)		Day: 2 471 865 Night: 2 791 373	
Per bin	Day	0.134	0.121	0.108	0.105	0.086	0.084	0.102	0.097
	Night	0.140	0.127	0.112	0.105	0.079	0.082	0.099	0.097
	Ratio	0.958	0.952	0.963	0.994	1.088	1.029	1.025	0.996
	Total	0.137	0.124	0.110	0.105	0.082	0.083	0.101	0.097
	Sample	18 011 (31 %)		2694 (5 %)		36 895 (64 %)		57 600	

the equator. The relationship is very low at higher latitudes. Regions of relatively high correlation are found near the west African coast, the Caribbean, Brazil, tropical Atlantic, central Sahara, southern Africa and southwest Asia. Aside from southern Africa, which is subject to spring and summer anthropogenic burning and absorbing smoke aerosols (e.g., Campbell et al., 2003), each of these regions are most commonly impacted by desert dusts, mostly Saharan, and, thus, a priori assignment of the lidar ratio for extinction retrieval is relatively consistent over time (e.g., Liu et al., 2008), though there is a body of work presently questioning the absolute magnitude of this value (Tesche et al., 2009, 2011; Wandinger et al., 2010). Central Sahara and southern Africa are also regions where NAAPS is known to be biased high versus AERONET (Reid et al., 2009), so these results are encouraging. Low correlation over oceans and at higher latitudes is understandable, given that the dynamic range of AOD is much lower than over land and nearer the equator (Figs. 3a, b, 4a and b).

Globally, RMSD (Fig. 4d) exceeds 0.1 over water and peaks over 0.25 over land per bin, which is a factor of at least two higher than that found between NAAPS and MODIS/MISR (Figs. 1c and 2c). As alluded to above, numbers of available data points per bin (Fig. 4e) are highest near the equator, despite an orbiting ground-track that is more favourable to high-latitude coverage (points lacking data in these composites are depicted as white and, thus, not reflected in the colour bars given). A similar pattern is found by Kittaka et al. (2011) when comparing CALIOP versus MODIS, thus, indicating that cloud cover is largely driving this relationship. However, compromised layer-identification and retrievals in low AOD scenarios at higher latitudes (i.e., relatively low particle backscatter coefficients within the column profile, wherein algorithm sensitivity is low) at higher latitudes, also potentially contributes.

CALIOP-to-NAAPS AOD ratios (Fig. 4f) indicate that the satellite retrievals are higher than the model across the southern oceans, in the Caribbean, Brazil, east Africa and Australia, but are generally lower elsewhere, though sample noise is again high at increasingly higher latitudes. From the per bin global averages in Table 1, CALIOP values are slightly higher within the global mean (0.099 vs. 0.097). Values are higher over land and coastal regions, but slightly lower over oceans. For all data points, however, NAAPS exceeds CALIOP globally (0.134 vs. 0.123), being higher over each surface regime.

Mean daytime 2007 QA CALIOP AOD retrievals (Fig. 5) depict the same major features as those derived during night, and are again consistent with corresponding daytime NAAPS data (Fig. 5b). These results are also consistent with both sets of global averages reported in Table 1. This finding is notable. The effects of ambient solar noise on CALIOP AOD retrievals are limited. Unlike the nighttime comparison above, NAAPS includes data from the sunlit sector of the model here, thus, consistent with the 00-h model analysis that benefits from concurrent MODIS/MISR assimilation. Correlation between CALIOP and NAAPS, however, remains relatively low (Fig. 5c). The highest relative correlation is found for the tropical Atlantic and eastern Caribbean. RMSD exhibits little variability (Fig. 5d) compared with results derived at night, though over-ocean values trend slightly higher. Numbers of available data points per grid bin again are highest near the equator (Fig. 5e).

Ratios of daytime CALIOP-to-NAAPS AOD (Fig. 5f) are slightly higher than night over the southern oceans, Caribbean and west/central Tropical Atlantic and most of the Pacific. However, the relationship is very difficult to characterise at high latitudes, from relatively low sample sizes. For the global per bin averages in Table 1, CALIOP AOD exceeds NAAPS (0.102 vs. 0.097), and the relationship holds

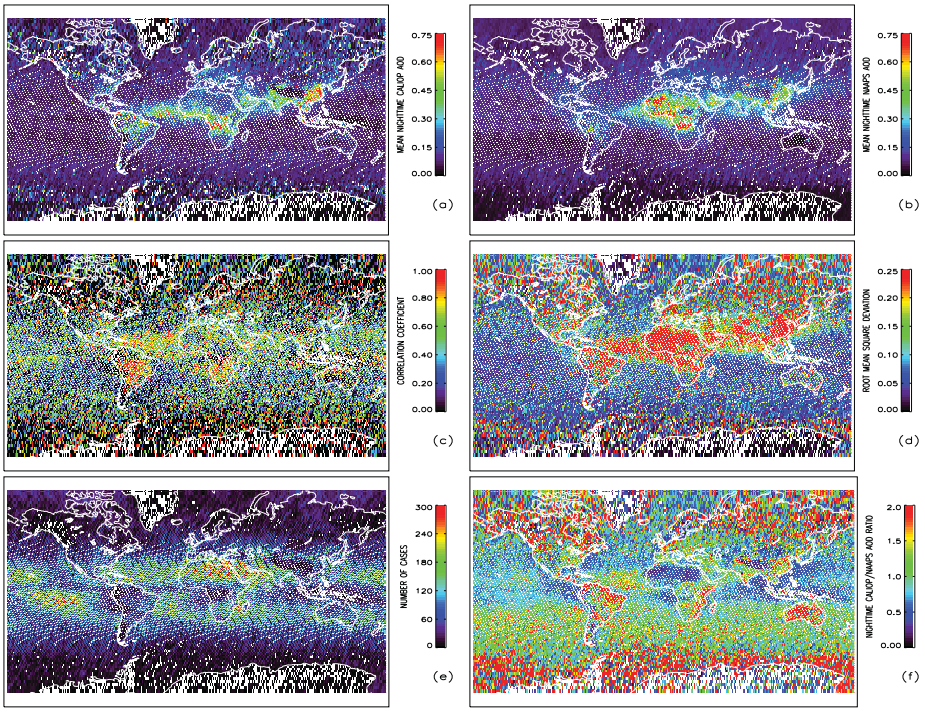

Fig. 4. For 2007 at 1° × 1° global resolution, **(a)** mean nighttime CALIOP 0.532 μm AOD, **(b)** corresponding mean nighttime NAAPS 0.550 μm AOD (see text), **(c)** correlation coefficient between the two datasets for all points inclusive, **(d)** root-mean-square deviation between the two, **(e)** number of corresponding cases per grid bin and **(f)** the ratio of corresponding mean nighttime CALIOP/NAAPS AOD. Points with no data coincide with a white pixel that is not represented on the colour bar.

for all three surface regimes. For all data points, however, NAAPS is again higher than CALIOP (0.132 vs. 0.126) in the global mean. This again holds for land, coast and ocean.

Shown in Fig. 6a are global composites of CALIOP day/night AOD ratio per bin, with corresponding results for NAAPS shown in Fig. 6b. As discussed above from Table 1, CALIOP day/night ratios exceed unity globally both for all data points and the per-bin normalised analysis (4.4 and 2.5 %, respectively). The relationship is reversed, however, when averaged globally per bin over land and coastal sites (0.134/0.108 vs. 0.140/0.112, respectively), which is seen most prominently in the composite image over the sub-tropical Atlantic Ocean and Europe. Maximum offsets per bin are ±20 % from these data, though this relationship is again sensitive to the dynamic range globally of AOD, discussed above, which complicates the analysis in regions where mean values are relatively low. The NAAPS day/night ratio, on the other hand, is less than unity when averaged globally for all data points (2.8 %) and very near 1.0 when averaged per bin (Table 1). Notable deviations from this latter standard are found in the composite image over the southern oceans and the southeastern Pacific, in general.

3.2 Sub-regional AOD assessments

Eight regions were selected for a comprehensive quantitative comparison of the 2007 QA CALIOP and NAAPS AOD datasets. Depicted on a global map in Fig. 7, these regions and their equivalent longitude/latitude start/end points are: North Atlantic (NA; 70° W/35° N–60° W/45° N), Caribbean (C; 65° W/10° N–55° W/20° N), Tropical Atlantic (TA; 35° W/15° N–25° W/25° N), Europe (E; 5° E/50° N–25° E/55° N), Arabian Sea (AS; 60° E/10° N–70° E/20° N), Southeast Asia (SEA; 100° E/10° N–110° E/20° N), South China Sea (SCS; 110° E/5° N–120° E/15° N) and Sea of Japan (SoJ; 130° E/35° N–140° E/45° N). Regional assignments and latitude/longitude points are also detailed in Tables 2–4, which include summaries of related AOD statistics derived for each domain, and are described in more specific detail below. Three regions are strictly over water (NA, TA, AS), three include some land and coastline, but are primarily over water (C, SCS, SoJ), and two are mostly over land (E and SEA).

Table 2 includes results derived within each sub-region for averaged 2007 5-km CALIOP QA sub-sample and corresponding NAAPS AOD from both night and day, retrieval uncertainty, RMSD, correlation coefficient, slope and coordinate of y-intercept for the linear regression between the two, median AOD, sample size and total available retrieval sample size. The ratio of the latter two parameters is considered a first-order proxy for regional cloud frequency. The primary findings from this analysis are:

Fig. 5. For 2007 at 1° × 1° global resolution, **(a)** mean daytime CALIOP 0.532 μm AOD, **(b)** corresponding mean daytime NAAPS 0.550 μm AOD (see text), **(c)** correlation coefficient between the two datasets for all points inclusive, **(d)** root-mean-square deviation between the two, **(e)** number of corresponding cases per grid bin and **(f)** the corresponding ratio of mean daytime CALIOP and NAAPS AOD. Points with no data coincide with a white pixel that is not represented on the colour bar.

1. Mean nighttime CALIOP AOD are lower than daytime values in five of the sub-regions (NA, C, AS, SEA and SCS) by as much as 20 %. In NA and C, NAAPS exhibits a day/night offset, though of not the same magnitude (approaching 10 %). In the others, NAAPS exhibits relative stability diurnally. This day/night offset from both datasets is generally consistent with the global averages of all data points and as normalised per bin, as described from Table 1.

2. CALIOP AOD retrieval uncertainties exhibit little day/night variance. Sample sizes, however, are very high regionally, thus, driving values low. No offset is found from further investigation of monthly and seasonal mean values (not shown), however. This is unusual considering the propagation of signal noise induced by solar background rates during daytime.

3. Mean CALIOP AOD are lower than that derived from NAAPS over water, except along the Saharan Dust Belt (C, TA, AS night), and high compared with the model over land. These offsets, approaching 50 % in the most extreme examples, exceed any expected difference between the two from wavelength difference. In every sub-region except AS, offsets are consistent from night to day. The slope of the linear correlation solved between CALIOP and NAAPS AOD is consistent in each sub-region with these findings. Regional land/ocean offsets are consistent with anomalies identified in other studies (Campbell et al., 2012b; Kittaka et al., 2011). From Table 1, CALIOP AOD are higher than NAAPS over land only when averaged globally per bin. For all data points, the relationship reverses. Over water, CALIOP is nearly 10 % lower over oceans (0.096 vs. 0.104) for all data points, but nearly equal when averaged globally per bin (0.082 vs. 0.083).

4. RMSD between CALIOP and NAAPS varies between 0.10 and 0.35 amongst the sub-regions, with no apparent difference between night and day.

5. Correlation between CALIOP and NAAPS varies between 0.20 and 0.75 within the sub-regions. The highest values are found in the sub-tropical Atlantic regions (C and TA). The lowest are found in the NA and SoJ regions, which are highest in latitude and two of the three lowest for mean AOD. Though no specific day/night dependency is clear, if anything, the data trend toward higher correlation during day, though degraded model skill inherent to the nighttime comparisons with NAAPS is likely influencing this relationship.

6. QA sample size relative to the complete Level 2 5-km NASA aerosol data product archive reflect rejection rates varying from 40–80 %. Day/night differences

Table 2. For 2007 and each sub-region defined, mean annual nighttime (Night) and daytime (Day) CALIOP aerosol optical depth (AOD), instrument/retrieval uncertainty (Unc.), corresponding mean annual NAAPS AOD, root-mean-square deviation between CALIOP and NAAPS, correlation coefficient between the two (Corl.), slope of the linear regression between the two (Slope), coordinate value of y-intercept solved from regression (Coord.), median of CALIOP AOD (Median) and sample size (Sample) and total number of available data files regardless of cloud-screening protocols described (Total).

	N. Atlantic 70° W/35° N–60° W/40° N		Caribbean 65° W/10° N–55° W/20° N		T. Atlantic 35° W/15° N–25° W/25° N		Europe 5° E/50° N–25° E/55° N		Arabian Sea 60° E/10° N–70° E/20° N		SE Asia 100° E/10° N–110° E/20° N		S. China Sea 110° E/5° N–120° E/15° N		Sea of Japan 130° E/35° N–140° E/45° N	
	Night	Day	Night	Day	Night	Day	Night	Day	Night	Day	Night	Day	Night	Day	Night	Day
CALIOP	0.077	0.102	0.177	0.207	0.234	0.214	0.208	0.178	0.236	0.277	0.341	0.385	0.087	0.099	0.153	0.147
Unc.	0.001	0.001	0.001	0.001	0.001	0.001	0.001	0.001	0.001	0.001	0.001	0.002	0.001	0.001	0.001	0.001
NAAPS	0.128	0.136	0.158	0.171	0.191	0.192	0.163	0.162	0.252	0.251	0.338	0.323	0.155	0.147	0.190	0.205
RMSD	0.123	0.143	0.177	0.177	0.223	0.159	0.229	0.184	0.186	0.181	0.328	0.327	0.122	0.107	0.183	0.188
Corl.	0.183	0.236	0.721	0.687	0.631	0.661	0.323	0.271	0.476	0.534	0.511	0.571	0.238	0.427	0.385	0.429
Slope	0.201	0.283	1.506	1.442	1.246	1.211	0.827	0.525	1.070	0.994	0.669	0.988	0.341	0.525	0.615	0.530
Coord.	0.051	0.064	−0.06	−0.04	−0.00	−0.02	0.073	0.093	−0.03	0.028	0.114	0.066	0.034	0.021	0.037	0.039
Median	0.057	0.069	0.088	0.118	0.130	0.147	0.129	0.129	0.178	0.233	0.209	0.263	0.067	0.072	0.091	0.095
Sample	3703	2736	11 039	8179	9691	10 174	5138	3798	11 248	8338	4729	2161	4999	2201	6308	4988
Total	6389	5398	19 049	17 810	15 737	18 614	10 494	7041	17 986	17 557	12 572	10 095	14 990	10 776	11 952	10 058

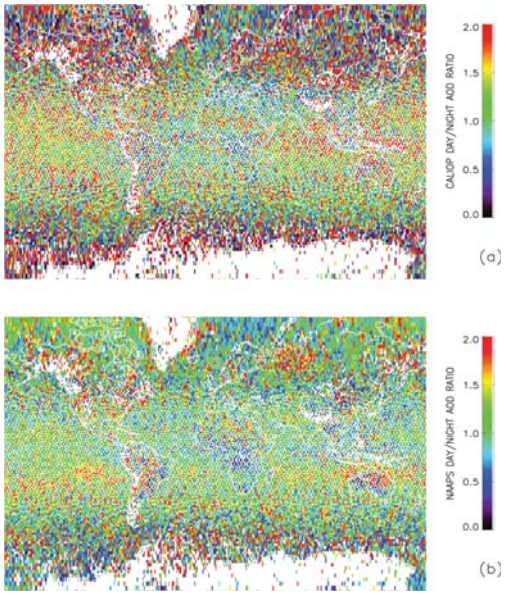

Fig. 6. Ratio of daytime versus nighttime AOD from 2007 for **(a)** CALIOP (0.532 μm) and **(b)** NAAPS (0.550 μm) for co-incident data points (see text). Points with no data coincide with a white pixel that is not represented on the colour bar.

in rejection increase nearing the equator, and particularly over the tropical Asian sub-regions (AS, SEA and SCS). Rejection rates likely increase due to cloud presence within the 5-km along-track averages, particularly in the latter regions from widespread regional convection that peaks during daytime (e.g., Reid et al., 2012). It is notable that relative differences between day/night AOD globally are reasonably small in light of differing sample sizes.

Kittaka et al. (2011) report global mean day and nighttime CALIOP AOD retrievals at 5° × 5° resolution for June, July and August 2006. Though their analysis is not specifically

Fig. 7. Depiction of the eight regions (North Atlantic, Caribbean, Tropical Atlantic, Europe, Arabian Sea, Southeast Asia, South China Sea and Sea of Japan) investigated for CALIOP versus NAAPS AOD comparisons.

quantitative on this point, interpretation of the global day versus night composites in their Fig. 1 indicates that nighttime AOD mostly exceed that retrieved during day over many regions. Their analysis focuses on Version 2.01 Level 2.0 Aerosol Layer data for points of co-incident daytime observation with Aqua-MODIS based on specific ground-track coupling metrics and, thus, fundamentally different than this one. Furthermore, their data screening is based only on variability in the prescribed lidar ratio at pre and post-processing stages, and for excluding aerosol layers where integrated attenuated backscatter exceeds 0.01 sr^{-1}. This difference raises question as to what degree do retrieval version, data screening and subsequent global averaging affect these analyses. Once reconciled, subsequent work must determine whether offsets represent physical or retrieval bias.

Following Table 2, Table 3 contains results of a supplemental reanalysis of the QA CALIOP sub-sample where only multiple contiguous AOD retrievals occurring along-track and corresponding within a common NAAPS grid bin are averaged and statistical day/night properties reassessed. Single data points are, thus, excluded. Such a "buddy-check" approach has been shown to reduce noise in passive-based

Table 3. As in Table 1, for all contiguous averages of CALIOP data segments occurring within the same NAAPS 1° × 1° grid bin.

	N. Atlantic 70° W/35° N–60° W/40° N		Caribbean 65° W/10° N–55° W/20° N		T. Atlantic 35° W/15° N–25° W/25° N		Europe 5° E/50° N–25° E/55° N		Arabian Sea 60° E/10° N–70° E/20° N		SE Asia 100° E/10° N–110° E/20° N		S. China Sea 110° E/5° N–120° E/15° N		Sea of Japan 130° E/35° N–140° E/45° N	
	Night	Day	Night	Day	Night	Day	Night	Day	Night	Day	Night	Day	Night	Day	Night	Day
CALIOP	0.084	0.111	0.188	0.204	0.246	0.235	0.226	0.194	0.248	0.292	0.347	0.385	0.089	0.101	0.166	0.162
Unc.	0.004	0.006	0.004	0.004	0.004	0.004	0.006	0.007	0.004	0.005	0.007	0.011	0.004	0.007	0.004	0.005
NAAPS	0.135	0.136	0.161	0.170	0.195	0.203	0.164	0.160	0.256	0.258	0.336	0.330	0.156	0.151	0.198	0.213
RMSD	0.113	0.144	0.152	0.136	0.194	0.135	0.211	0.193	0.159	0.153	0.282	0.290	0.107	0.101	0.160	0.176
Corl.	0.239	0.221	0.825	0.794	0.724	0.792	0.382	0.205	0.622	0.623	0.623	0.625	0.311	0.490	0.462	0.461
Slope	0.180	0.274	1.616	1.439	1.278	1.287	0.898	0.384	1.247	0.990	0.784	0.899	0.344	0.539	0.619	0.529
Coord.	0.060	0.074	−0.07	−0.04	−0.00	−0.03	0.078	0.133	−0.07	0.036	0.084	0.088	0.035	0.026	0.044	0.049
Median	0.066	0.079	0.097	0.121	0.132	0.169	0.151	0.147	0.193	0.245	0.236	0.267	0.072	0.087	0.106	0.111
Sample	436	342	1040	871	1035	1068	669	519	937	799	531	267	509	291	732	597

Table 4. As in Tables 1 and 2, for those contiguous averages of CALIOP data segments containing at least 6 AOD values, where the highest and lowest 25 % of the data are rejected and the median 50 % analysed.

	N. Atlantic 70° W/35° N–60° W/40° N		Caribbean 65° W/10° N–55° W/20° N		T. Atlantic 35° W/15° N–25° W/25° N		Europe 5° E/50° N–25° E/55° N		Arabian Sea 60° E/10° N–70° E/20° N		SE Asia 100° E/10° N–110° E/20° N		S. China Sea 110° E/5° N–120° E/15° N		Sea of Japan 130° E/35° N–140° E/45° N	
	Night	Day	Night	Day	Night	Day	Night	Day	Night	Day	Night	Day	Night	Day	Night	Day
CALIOP	0.075	0.100	0.174	0.210	0.234	0.210	0.193	0.165	0.242	0.274	0.339	0.402	0.086	0.094	0.148	0.139
Unc.	0.005	0.007	0.004	0.005	0.005	0.005	0.007	0.008	0.005	0.006	0.008	0.015	0.004	0.008	0.005	0.006
NAAPS	0.127	0.136	0.158	0.172	0.193	0.191	0.163	0.160	0.254	0.251	0.334	0.328	0.152	0.145	0.189	0.204
RMSD	0.100	0.120	0.131	0.143	0.178	0.107	0.172	0.123	0.159	0.139	0.294	0.287	0.101	0.077	0.141	0.155
Corl.	0.295	0.341	0.826	0.788	0.716	0.773	0.376	0.417	0.559	0.639	0.571	0.695	0.320	0.660	0.507	0.558
Slope	0.234	0.341	1.484	1.468	1.210	1.132	0.746	0.573	1.119	0.989	0.728	1.206	0.346	0.554	0.687	0.556
Coord.	0.046	0.054	−0.06	−0.04	0.001	−0.01	0.071	0.073	−0.04	0.027	0.096	0.007	0.033	0.014	0.018	0.026
Median	0.063	0.070	0.089	0.126	0.131	0.155	0.131	0.132	0.191	0.236	0.225	0.281	0.069	0.077	0.094	0.098
Sample	272	204	812	610	731	757	384	281	767	598	367	161	361	162	472	385

satellite AOD retrievals (Zhang and Reid, 2006), and is designed to both lessen the influence of sample/instrument noise, and to increase spatial representativeness relative to the offset of the CALIOP observations to the NAAPS grid bin centre. Each average is treated as a single point, not a weighted one.

From this newly-averaged sample, CALIOP and NAAPS AOD for the C sub-region are displayed for day and night in Fig. 8, including all data points (Fig. 8a), those CALIOP averages including two or more contiguous data points (Fig. 8b), averages of six or more consecutive points (Fig. 8c), eleven or more (Fig. 8d) and sixteen or more (Fig. 8e). Given the 98.2° inclination angle of the CALIPSO near-polar orbit, its ground-track at the equator intersecting a single NAAPS grid-bin can include as many as twenty-two consecutive 5-km L2-APprof profiles, based on assignment of a 5-km CALIOP QA profile to NAAPS bin at the mid-point of the along-track average and 112.47 km per degree of latitude (e.g., Campbell et al., 2010).

Little change is found between Tables 2 and 3. Mean nighttime CALIOP AOD remain lower than the daytime mean in the same five sectors as above. AOD retrieval uncertainties show little difference between night and day, except in NA, SEA and SCS. Mean CALIOP AOD relative to NAAPS exhibit the same land/ocean offsets, including over the Saharan Dust Belt sub-region. Correlation and the slope of the linear regression between the two datasets exhibit no statistically significant changes. RMSD drops slightly to between 0.10 and 0.30. At increasingly longer data averages in the C sub-region (Fig. 8), correlation coefficient increases and the slope of the linear regression mostly decreases up to the inclusion of eleven or more data points (Fig. 8d). When sixteen or more points are included, daytime correlation recedes slightly, nighttime increases very slightly and both slopes increase, which likely reflects the growing influence of aerosol autocorrelation lengths and representativeness bias for averages of 80 km or more (Anderson et al., 2003; Zhang et al., 2008). In this instance, the overestimate of AOD in the C sub-region by CALIOP compared with NAAPS appears, again, systemic.

Results of a third and final analysis are shown in Table 4. Here, only contiguous along-track data averages coinciding with the same NAAPS grid bin and containing at least six data points are used. However, the lowest and highest 25 % of those CALIOP data points making up the average are rejected. The purpose of this screening is to isolate the mode within the data distribution that best represents algorithm performance, excludes noise and potentially unfiltered cloud bias, and is less subject to random error. Notably, CALIOP AOD increase relative to NAAPS, compared with Tables 2 and 3, exceeding the model in C, TA, E, AS day and SEA. Correlation mostly increases, varying now between 0.30 and 0.85, though relative decreases occur in some sub-regions (i.e., SEA night). Linear regression slopes

Table 5. For each sub-region defined beginning in Table 1, the mean height for both day and night corresponding with the 0.01, 0.001 and 0.0001 km^{-1} isopleth for CALIOP-derived 0.532 μm extinction coefficient. A * denotes the presence of multiple layers and, hence, the corresponding mean height for the lowest such layer. Cases where the isopleth height exceeded 10.0 km m.s.l. are denoted with "N/A".

	Day			Night		
	0.01 km^{-1}	0.001 km^{-1}	0.0001 km^{-1}	0.01 km^{-1}	0.001 km^{-1}	0.0001 km^{-1}
N. Atlantic 70° W/35° N–60° W/40° N	1.8	3.7	4.2*	2.0	4.0*	n/a
Caribbean 65° W/10° N–55° W/20° N	3.8	4.8	5.1	3.4	4.6	5.3
T. Atlantic 35° W/15° N–25° W/25° N	4.2	5.4	6.2	4.5	5.6	6.3
Europe 5° E/50° N–25° E/55° N	2.5	3.7	4.6*	2.5	4.1	6.2
Arabian Sea 60° E/10° N–70° E/20° N	4.1	5.1	5.5	3.9	5.2	5.8*
SE Asia 100° E/10° N–110° E/20° N	3.4	4.5	4.8	3.4	4.3	5.0
South China Sea 110° E/5° N–120° E/15° N	1.9	2.5	3.6	1.8	4.0	4.2*
Sea of Japan 130° E/35° N–140° E/45° N	2.9	5.0	9.9	3.4	7.3	n/a

trend slightly closer to unity and RMSD improves in all subsectors except SEA. Some performance criteria improve with averaging and careful sample selection. Systematic retrieval offsets, however, persist.

3.3 How representative is the day/night CALIOP vertical extinction coefficient profile?

Mean CALIOP 0.532 μm aerosol particle extinction coefficient profiles with corresponding error bars, solved by interpolating the 60 m 2007 QA sub-sample to a 100 m vertical grid, are shown annually for the C sub-region in Fig. 9 for day, night and the aggregate mean (Fig. 9a), the March–May seasonal average (MMA; Fig. 9b), June–August (JJA; Fig. 9c), September–November (SON; Fig. 9d) and December–February (DJF; Fig. 9e). For comparison, corresponding mean Level 2.0 aerosol extinction coefficient profiles with uncertainties are shown as derived from the Micropulse Lidar Network (MPLNET; Welton et al., 2001) 0.532 μm instrument at Barbados (13.17° N, 59.43° W, 30 m m.s.l.) for data collected from August 2008 through June 2011. Additionally, for the JJA composite, the mean Level 2.0 0.523 μm extinction coefficient profile with corresponding error bars is shown from an MPLNET instrument deployed for the June–July 2000 Puerto Rican Dust Experiment at Roosevelt Roads Naval Station, Puerto Rico (18.22° N, 65.60° W, 6 m m.s.l.; Reid et al., 2003).

MPLNET extinction retrievals are based on a single-channel elastic-scattering measurement, like CALIOP. However, inversion of the processed signal is constrained by AOD measurements made with a co-located AERONET sun photometer, and a layer-mean lidar ratio is solved as an intermediate processing step (e.g., Welton et al., 2002). Mean 2007 total annual CALIOP 0.532 μm AOD at C is 0.188, whereas NAAPS 0.550 μm AOD is 0.164. At Barbados, the corresponding AERONET-integrated mean annual 0.532 μm AOD

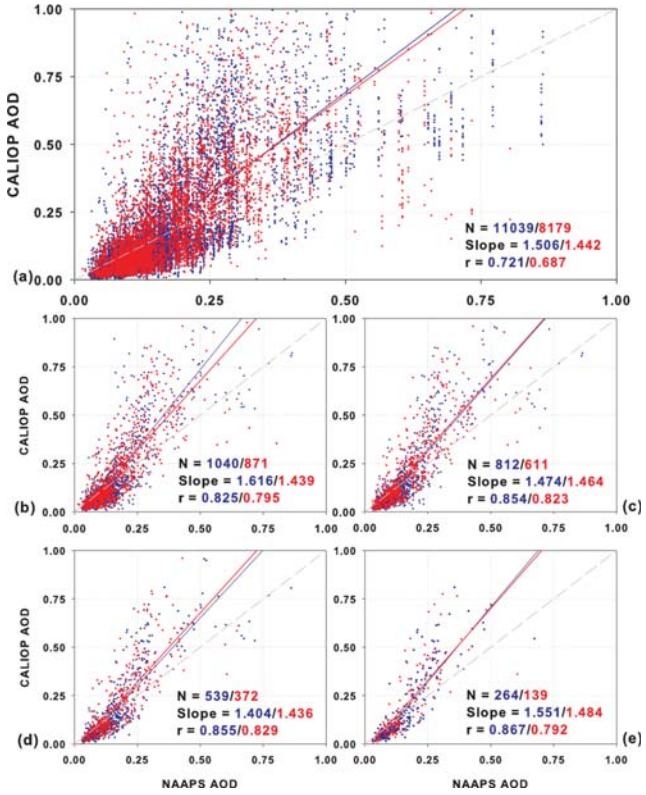

Fig. 8. In 2007 for Caribbean sector (65° W/10° N to 55° W/20° N), **(a)** all CALIOP 0.532 μm AOD versus corresponding 1° × 1° 0.550 μm NAAPS AOD during night (blue) and day (red), with number of data points, linear regression slope and correlation coefficient, *r*, given in the inset; **(b)** same but for averages of CALIOP along-track 0.532 μm AOD in segments of 2–5 data points occurring within the same NAAPS grid bin; **(c)** same for averages of 6–10 such consecutive data points; **(d)** 11–15 data points; **(e)** ≥ 16 data points.

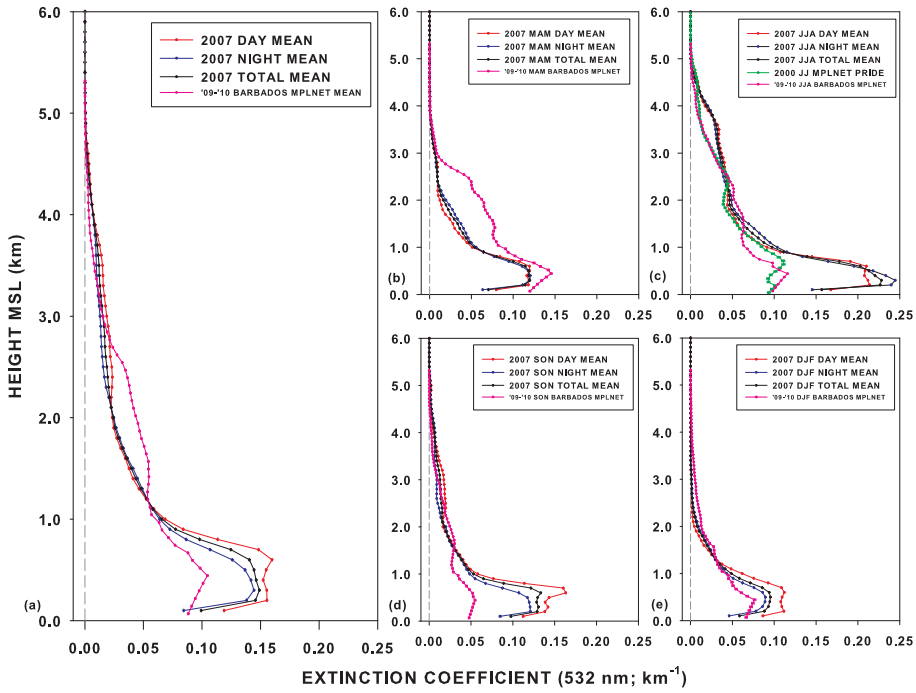

Fig. 9. In 2007 for Caribbean sector (65° W/10° N to 55° W/20° N), **(a)** mean daytime, nighttime and total 0.532 µm CALIOP extinction coefficient profiles (see inset) and mean Micropulse Lidar Network (MPLNET) Level 2.00.532 µm extinction coefficient profile collected at Barbados (13.17° N, 59.43° W, 30 m m.s.l.) for August 2008–June 2011; **(b)** March-to-May three-monthly average of 2007 CALIOP mean day, night and total 0.532 µm extinction coefficient profile versus corresponding three-monthly average of Barbados MPLNET data from 2009–2011; **(c)** June–August three-monthly average of 2007 CALIOP mean day, night and total 0.532 µm extinction coefficient profile versus mean Level 2.0 0.523 µm extinction coefficient profile derived for June–July 2000 at MPLNET/Roosevelt Roads Naval Station, Puerto Rico site (18.22° N, 65.60° W, 6 m m.s.l.) and for Barbados from 2009–2011; **(d)** same as **(b)** now for September-to-November; **(e)** same as **(b)** and **(d)** now for December-to-February.

for the MPLNET Level 2.0 data period is 0.174, and 0.211 during JJA. The Roosevelt Roads mean for June–July 2000 is 0.208. The Puerto Rican MPLNET dataset has been studied previously (e.g., Livingston et al., 2003; Reid et al., 2003). As some representativeness bias is present in these comparisons (e.g., Kovacs, 2006), they are presented strictly for qualitative interpretation.

CALIOP and MPLNET mean annual profiles depict a common layer depth, and are mostly similar in vertical distributions. Below 1.0 km m.s.l., CALIOP is higher, and MPLNET is higher between 1.0 and 2.5 km m.s.l. CALIOP indicates slightly more extinction present above 2.5 km m.s.l., as well. Below 1.0 km m.s.l., calibration for optical overlapping in the MPL receiver system is sensitive at heights nearest the instrument (Campbell et al., 2002). MPLNET retrievals of extinction have been shown effective and robust, however, throughout the aerosol particle profile when compared with other lidars, including Raman-based instruments and airborne measurement techniques (Schmid et al., 2006). Greater disparity is present within the seasonal profiles. MPLNET resolves a greater elevated layer component at Barbados above 1.0 km m.s.l. during MAM, less extinction above 2.5 km m.s.l. during JJA and lower values below 1.0 km m.s.l. during JJA, SON and DJF. The 2000 Roosevelt Roads mean profile matches very well with that from Barbados during JJA.

In Fig. 10, fractional partitioning of extinction as a function of the seven discrete aerosol species used in HERA for parameterizing the a priori lidar ratio value in the CALIOP retrieval is shown for the mean 2007 annual and JJA profiles. This analysis indicates that "polluted dust" contributes most at C below 1.0 km m.s.l. During JJA (Fig. 10b), when near-surface magnitudes are highest annually, the fractional contribution of "polluted dust" dominates CALIOP extinction at these heights. The a priori lidar ratio used for "polluted dust" is 55 sr, versus 40 sr for "dust" and 20 sr for "clean marine" (Omar et al., 2009). This relatively absorptive aerosol particle type may bias values high relative to the selection of these two other less-absorptive aerosol particle types, which are common to the regional C marine boundary layer (Li-Jones and Prospero, 1999). As context, the layer-mean lidar ratio solved in MPLNET Level 2.0 retrievals at Barbados was 31.4 annually and 31.0 during JJA. At Roosevelt Roads, it was 53.1.

The daytime CALIOP aerosol particle extinction coefficient profile exhibits higher values during daytime at C

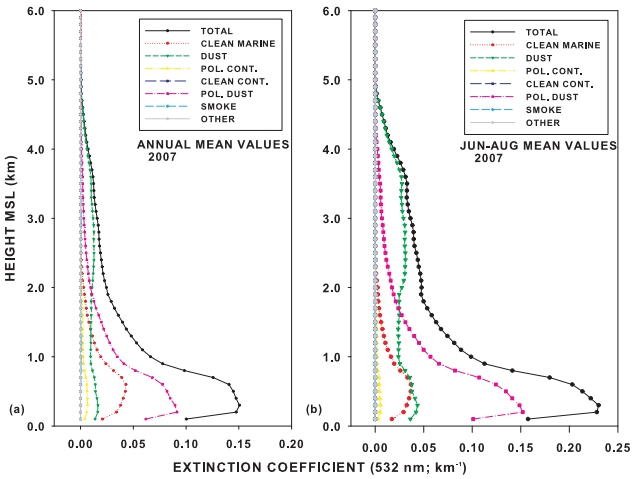

Fig. 10. Corresponding with both the **(a)** 2007 total mean annual profile in Fig. 9a and **(b)** June–August 2007 three-monthly averaged one in Fig. 9c, the fractional contribution to total extinction coefficient for each of the seven possible species identified and, thus, parameterized for lidar extinction-to-backscatter ratio, in CALIOP aerosol retrievals (see inset).

than night, which is consistent with generally higher daytime AOD found globally discussed above. In spite of this, as seen from Fig. 9, the mean particle layer top height solved during night matches well with that from day. This is surprising given both the AOD difference combined with the effects of solar background noise, which might be expected to limit daytime identification of diffuse/optically-thin aerosol particles common near and above the top of the surface-detached aerosol layer.

In Table 5, the height of the 0.01, 0.001 and 0.0001 km^{-1} isopleth found from each sub-regional mean 0.532 μm CALIOP extinction coefficient profile for both day and night is reported. At C, heights are 3.8, 4.8 and 5.1 km m.s.l., respectively, during daytime, compared with 3.4, 4.6 and 5.3 km m.s.l. at night. In the other sub-regions at the 0.01 and 0.001 km^{-1} thresholds, mean heights are relatively consistent except for SCS and SoJ. At 0.0001 km^{-1} resolution, however, significant offsets are found, which are believed consistent with optimised nighttime sensitivities. Therefore, to within a few hundred metres, CALIOP layer-identification and mean layer top height is relatively stable diurnally, save for the most optically-thin (i.e., negligible) segments of the particle profile.

The sum total of particle layers identified in CALIOP retrievals at night exceeds that found during daytime by more than 50 % despite lower mean AOD (not shown). Somewhat paradoxically then, and in closing, higher AOD are found during daytime in spite of fewer total layers, but with a common mean effective layer top height. Future study is necessary to reconcile this finding. One plausible cause relates to the sensitivity of layer-identification thresholds between day/night for resolving clear sky gaps within diffuse/optically-thin layers (e.g., Campbell et al., 2008). At night, improved sensitivity and algorithm/logical compliance identifying clear-sky gaps can yield lower AOD compared with daytime, where apparent gaps and inherent noise are integrated within the column solution. However, note that in the annual mean at C (Fig. 9a), the bulk of the AOD offset is induced nearest the surface within a segment of highest values for extinction coefficient. This suggests that in this case another mechanism may be occurring, including day/night differences in layer base identification by the algorithms or simple physical decoupling in the boundary layer from surface source forcing (e.g., Osborne et al., 2000).

4 Conclusions and impact

NASA Cloud Aerosol Lidar with Orthogonal Polarization (CALIOP) Version 3.01 5-km quality-assured (QA) retrievals of 0.532 μm aerosol optical depth (AOD) from 2007 are evaluated during nighttime at 1° × 1° resolution relative to 0.550 μm analyses made by a global aerosol transport model equipped with two-dimensional variational assimilation of quality-assured NASA Moderate Resolution Imaging Spectroradiometer (MODIS) and Multi-angle Imaging Spectroradiometer (MISR) AOD. The *US Navy Aerosol Analysis and Prediction System* (NAAPS) generates global forecasts for aerosol visibility every six hours out to six days. NAAPS AOD analyses used to validate CALIOP retrievals reflect a nominal 12-h model forecast due to lack of MODIS/MISR data for assimilation within the dark sector of the model at initialisation. The model is shown to exhibit reasonable stability, however, between the 00-h analysis and 24-h forecast when compared with MODIS/MISR, thus, ensuring representativeness for this study. In the absence of sunlight, since passive radiometric AOD retrievals rely overwhelmingly on scattered radiances, the model represents one of the few practical global estimates available from which to attempt such an evaluation. Daytime comparisons of CALIOP and NAAPS are described as supplemental context for the nighttime study. Global composites of CALIOP and NAAPS AOD are shown, as well as statistical analyses for eight regional domains. Averaged vertical profiles of 0.532 μm CALIOP extinction coefficient versus ground-based elastic-scattering lidar retrievals are shown, as well as fractional contribution to total AOD for each of the seven distinct aerosol models used for assigning the a priori lidar ratio used in solving CALIOP extinction.

The primary findings of this study are:

1. Mean nighttime CALIOP AOD are in nearly all cases lower than daytime values (0.121 vs. 0.126 for all aggregated data points, and 0.099 vs. 0.102 when averaged per grid bin, both globally), though the relationship is reversed when analysed in a per-bin average over land and coastal regions (0.134/0.108 vs. 0.140/0.112, respectively). Though the magnitude of the offset varies

regionally, maximums per bin approach 20 %. Prominent regions where nighttime AOD exceeds daytime include the sub-tropical Atlantic Ocean and Europe. AOD uncertainties exhibit day/night variability in only a limited number of global regions, and only when along-track averaging and sample-filtering of high-variance data points are applied.

2. When globally averaged per 1° × 1° grid bin, CALIOP AOD are higher over land versus NAAPS (0.137 vs. 0.124). Over water, the two datasets are nearly equal (0.082 vs. 0.083). For all data points inclusive, NAAPS exceeds CALIOP over all surface types (land, coastal and ocean). When analysed for eight distinct sub-regions, CALIOP exceeds NAAPS over land, though the relationship does not hold over open waters near the Sahara region that are frequently subject to dust transport. Differences exceed that expected for the slight wavelength difference between the two datasets, approaching 50 % in extreme cases. Regional land/ocean offsets in CALIOP AOD are consistent with those identified in previous studies (Campbell et al., 2012b; Kittaka et al., 2011).

3. Correlation between 5-km CALIOP AOD and corresponding NAAPS data points is relatively low globally during both day and night except for Saharan dust transport zones over the Tropical Atlantic and Caribbean, where correlation approaches 0.8. Along-track averaging and sample filtering, described above, improve this and other statistical methods described for assessing CALIOP retrieval skill (i.e., root-mean-square deviation and the slope of the linear regression). However, whereas further averaging and data screening improve these statistical metrics, systemic biases, such as high/low land/water and high day versus night AOD relative to NAAPS persist, indicating that the offsets are systemic.

4. Annual and seasonal mean vertical profiles 0.532 μm for aerosol particle extinction coefficient compare well with ground-based 0.523 μm and 0.532 μm elastic-scattering lidar retrievals collected at two sites. Offsets and their variability regionally are likely due to irregularities in the a priori selection of the lidar extinction-to-backscatter ratio necessary for conducting iterative elastic-scattering CALIOP retrievals of 0.532 μm aerosol particle extinction coefficient. An example of such irregularity is shown from the Caribbean, where selection of a relatively absorptive aerosol particle model type is likely inducing a higher mean extinction coefficient near the surface than is present. It is undetermined how this effect is manifested with the global averages.

5. Although daytime AOD are generally higher than nighttime values, effective CALIOP-derived layer top heights are comparable (significant variance found for only the most optically-thin/diffuse segments of mean extinction coefficient profiles), despite more total particle layers being identified during night. Further study is necessary to reconcile this scenario.

Overall, the results of this study demonstrate that nighttime CALIOP datasets are reasonably consistent with daytime retrievals. This finding is impressive given the negative influence of ambient solar noise on lidar retrievals at visible wavelengths, particularly for single-channel elastic-scattering instruments, for which extinction is retrieved indirectly (e.g., Young and Vaughan, 2009). Kittaka et al. (2011) note that differences are to be expected between night and daytime datasets due to variability in systematic calibration errors, instrument sensitivities in day and nighttime sky conditions and diurnal changes to the aerosol. The systematic offset between day and nighttime AOD is a topic that requires further study in order to reconcile previous versions, and motivate future iterations, of the Level 2 data archive. Still, whereas many important characteristics of the CALIOP datasets have been identified and reported relative to NAAPS datasets, and are summarised above, perhaps the more important conclusion from this study is that CALIOP Version 3.01 retrieval performance is stable throughout the diurnal cycle, which is a notable achievement for the mission science team, and an important performance metric for investigators tasked with applying these data for climate study.

In closing, this paper indirectly serves as a starting point for a global investigation of the efficacy of CALIOP retrievals of aerosol optical properties. Though not the intention of this work, in applying NAAPS as the contextual basis for evaluating day versus night performance some offsets exist in the comparisons/tables that are likely attributable to systemic biases in either dataset. For example with NAAPS, since the model covaries so highly with its passively-retrieved satellite assimilation inputs, skill depreciates in regions where surface brightness is heterogeneous (e.g., deserts, coastal regions, etc. . . . ; Zhang and Reid, 2009). Further, in source regions, the model can struggle with plume injection, which subsequently impacts AOD analysis (e.g., Xian et al., 2009). The use of parameterized aerosol optical models with CALIOP algorithms, can similarly lead to relatively high uncertainties and/or bias, which is a topic that is now receiving necessary mechanistic scrutiny in more limited regional settings (e.g., Campbell et al., 2012b). These evaluations, however, serve the constructive purpose of highlighting logical gaps that can be improved in future iterations of the CALIOP algorithms and overall data archive. The results here, though some inconsistencies are clear, are qualitatively stable. Any efforts that can strengthen the retrievals, ultimately, will both positively impact CALIOP research and its legacy, but also positively influence mission planners and algorithm teams assigned future elastic-scattering lidar instruments.

Acknowledgements. This research was funded by the Office of Naval Research Code 35. Author JRC acknowledges the support of NASA Interagency Agreement NNG11HG12I, on behalf of the Micropulse Lidar Network. The group acknowledges the NASA AERONET programme, their contributing principal investigators and staff for coordinating the coastal and inland sites and datasets used in this study.

Edited by: V. Amiridis

References

Amiridis, V., Giannakaki, E., Balis, D. S., Gerasopoulos, E., Pytharoulis, I., Zanis, P., Kazadzis, S., Melas, D., and Zerefos, C.: Smoke injection heights from agricultural burning in Eastern Europe as seen by CALIPSO, Atmos. Chem. Phys., 10, 11567–11576, doi:10.5194/acp-10-11567-2010, 2010.

Anderson, T. L., Charlson, R. J., Winker, D. M., Ogren, J. A., and Holmén, K.: Mesoscale Variations of Tropospheric Aerosols, J. Atmos. Sci., 60, 119–136, 2003.

Bessagnet, B., Menut, L., Aymoz, G., Chepfer, H., and Vautard, R.: Modeling dust emissions and transport within Europe: The Ukraine March 2007 event, J. Geophys. Res., 113, D15202, doi:10.1029/2007JD009541, 2008.

Campbell, J. R., Hlavka, D. L., Welton, E. J., Flynn, C. J., Turner, D. D., Spinhirne, J. D., Scott, V. S., and Hwang, I. H.: Full-time, eye-safe cloud and aerosol lidar observation at Atmospheric Radiation Measurement program sites: instruments and data analysis, J. Atmos. Ocean. Tech., 19, 431–442, 2002.

Campbell, J. R., Welton, E. J., Spinhirne, J. D., Ji, Q., Tsay, S.-C., Piketh, S. J., Barenbrug, M., and Holben, B. N.: Micropulse Lidar observations of tropospheric aerosols over northeastern South Africa during the ARREX and SAFARI-2000 Dry Season experiments, J. Geophys. Res., 108, 8497, doi:10.1029/2002JD002563, 2003.

Campbell, J. R., Sassen, K., and Welton, E. J.: Elevated cloud and aerosol layer retrievals from micropulse lidar signal profiles, J. Atmos. Ocean. Tech., 25, 685–700, 2008.

Campbell, J. R., Reid, J. S., Westphal, D. L., Zhang, J., Hyer, E. J., and Welton, E. J.: CALIOP aerosol subset processing for global aerosol transport model data assimilation, IEEE J. Sel. Top. Appl., 3, 203–214, doi:10.1109/JSTARS.2010.2044868, 2010.

Campbell, J. R., Welton, E. J., Krotkov, N. A., Stewart, S. A., Yang, K., and Fromm, M. D.: Likely seeding of cirrus clouds by stratospheric Kasatochi volcanic aerosol particles near a mid-latitude tropopause fold, Atmos. Environ., 46, 441–448, doi:10.1016/j.atmosenv.2011.09.027, 2012a.

Campbell, J. R., Reid, J. S., Westphal, D. L., Zhang, J., Tackett, J. L., Chew, B. N., Welton, E. J., Shimizu, A., Sugimoto, N., Aoki, K., and Winker, D. M.: Characterizing the vertical profile of aerosol particle extinction and linear depolarization over Southeast Asia and the Maritime Continent: the 2007–2009 view from CALIOP, Atmos. Res., online first: doi:10.1016/j.atmosres.2012.05.007, 2012b.

Carn, S. A., Krueger, A. J., Krotkov, N. A., Yang, K., and Evans, K.: Tracking volcanic sulfur dioxide clouds for aviation hazard mitigation, Nat. Hazards, 51, 325–343, doi:10.1007/s11069-008-9228-4, 2009.

Diner, D. J., Beckert, J. C., Bothwell, G. W., and Rodriguez, J. I.: Performance of the MISR instrument during its first 20 months in earth orbit, IEEE T. Geosci. Remote, 40, 1449–1466, doi:10.1109/TGRS.2002.801584, 2002.

Fromm, M., Lindsey, D. T., Servranckx, R., Yue, G., Trickl, T., Sica, R., Doucet, T., and Godin-Beekman, S.: The untold story of pyrocumulonimbus, B. Am. Meteorol. Soc., 91, 1193–1209, doi:10.1175/2010BAMS3004.1, 2010.

Holben, B. N., Eck, T. F., Slutsker, I., Tanré, D., Buis, J. P., Setzer, A., Vermote, E., Reagan, J. A., Kaufman, Y. J., Nakajima, T., Lavenu, F., Jankowiak, I., and Smirnov, A.: AERONET – A Federated Instrument Network and Data Archive for Aerosol Characterization, Remote Sens. Environ., 66, 1–16, 1998.

Hsu, N. C., Tsay, S.-C., King, M. D., and Herman, J. R.: Aerosol properties over bright-reflecting source regions, IEEE T. Geosci. Remote, 47, 557–569, 2004.

Hunt, W. H., Winker, D. M., Vaughan, M. A., Powell, K. A., Lucker, P. L., and Weimer, C.: CALIPSO Lidar Description and Performance Assessment, J. Atmos. Ocean. Tech., 26, 1214–1228, 2009.

Hyer, E. J., Reid, J. S., and Zhang, J.: An over-land aerosol optical depth data set for data assimilation by filtering, correction, and aggregation of MODIS Collection 5 optical depth retrievals, Atmos. Meas. Tech., 4, 379–408, doi:10.5194/amt-4-379-2011, 2011.

Kacenelenbogen, M., Vaughan, M. A., Redemann, J., Hoff, R. M., Rogers, R. R., Ferrare, R. A., Russell, P. B., Hostetler, C. A., Hair, J. W., and Holben, B. N.: An accuracy assessment of the CALIOP/CALIPSO version 2/version 3 daytime aerosol extinction product based on a detailed multi-sensor, multi-platform case study, Atmos. Chem. Phys., 11, 3981–4000, doi:10.5194/acp-11-3981-2011, 2011.

Kahn, R. A., Garay, M. J., Nelson, D. L., Yau, K. K., Bull, M. A., Gaitley, B. J., Martonchik, J. V., and Levy, R. C.: Satellite-derived aerosol optical depth over dark water from MISR and MODIS: Comparisons with AERONET and implications for climatological studies, J. Geophys. Res., 112, D18205, doi:10.1029/2006JD008175, 2007.

Kahn, R. A., Nelson, D. L., Garay, M. J., Bull, M. A., Diner, D. J., Martonchik, J. V., Paradise, S. R., Hansen, E. G., and Remer, L. A.: MISR aerosol product attributes and statistical comparisons with MODIS, IEEE T. Geosci. Remote, 47, 4095–4114, doi:10.1109/TGRS.2009.2023115, 2009.

Kittaka, C., Winker, D. M., Vaughan, M. A., Omar, A., and Remer, L. A.: Intercomparison of column aerosol optical depths from CALIPSO and MODIS-Aqua, Atmos. Meas. Tech., 4, 131–141, doi:10.5194/amt-4-131-2011, 2011.

Kovacs, T.: Comparing MODIS and AERONET aerosol optical depth at varying separation distances to assess ground-based validation strategies for spaceborne lidar, J. Geophys. Res., 111, D24203, doi:10.1029/2006JD007349, 2006.

Li-Jones, X. and Prospero, J. M.: Variations in the size distribution of non-sea-salt sulfate aerosol in the marine boundary layer at Barbados: Impact of African dust, J. Geophys. Res., 103, 16073–16084, 1999.

Liu, Z., Hunt, W., Vaughan, M., Hosteller, C., McGill, M., Powell, K., Winker, D., and Hu, Y.: Estimating random errors due to shot noise in backscatter lidar observations, Appl. Optics, 45, 4437–4447, 2006.

Liu, Z., Omar, A., Vaughan, M., Hair, J., Kittaka, C., Hu, Y., Powell, K., Trepte, C., Winker, D., Hostetler, C., Ferrare, R., and Pierce, R.: CALIPSO lidar observations of the optical properties of Saharan dust: A case study of long-range transport, J. Geophys. Res., 113, D07207, doi:10.1029/2007JD008878, 2008.

Liu, Z., Vaughan, M., Winker, D., Kittaka, C., Getzewich, B., Kuehn, R., Omar, A., Powell, K., Trepte, C. and Hostetler, C.: The CALIPSO Lidar Cloud and Aerosol Discrimination: Version 2 Algorithm and Initial Assessment of Performance, J. Atmos. Ocean. Tech., 26, 1198–1213, 2009.

Liu, Z., Winker, D., Omar, A., Vaughan, M., Trepte, C., Hu, Y., Powell, K., Sun, W., and Lin, B.: Effective lidar ratios of dense dust layers over North Africa derived from the CALIOP measurements, J. Quant. Spectrosc. Ra., 112, 204–213, doi:10.1016/j.jqsrt.2010.05.006, 2011.

Livingston, J. M., Russell, P. B., Reid, J. S., Redemann, J., Schmid, B., Allen, D. A., Torres, O., Levy, R. C., Remer, L. A., Holben, B. N., Smirnov, A., Dubovik, O., Welton, E. J., Campbell, J. R., Wang, J., and Christopher, S. A.: Airborne sun photometer measurements of aerosol optical depth and columnar water vapor during the Puerto Rico Dust Experiment, and comparison with land, aircraft, and satellite measurements, J. Geophys. Res., 108, 8588, doi:10.1029/2002JD002520, 2003.

Martonchik, J. V., Diner, D. J., Kahn, R., Gaitley, B., and Holben, B. N.: Comparison of MISR and AERONET aerosol optical depths over desert sites, Geophys. Res. Lett., 31, L16102, doi:10.1029/2004GL019807, 2004.

National Aeronautics and Space Administration Cloud-Aerosol LIDAR Infrared Pathfinder Satellite Observations (CALIPSO), data management system, data products catalog, PC-SCI-503, Release 3.2, Langley Research Center, Hampton Virginia, 84 pp., 2010.

Omar, A. H., Winker, D. M., Kittaka, C., Vaughan, M. A., Liu, Z., Hu, Y., Trepte, C. R., Rogers, R. R., Ferrare, R. A., Lee, K.-P., Kuehn, R. E., and Hostetler, C. A.: The CALIPSO Automated Aerosol Classification and Lidar Ratio Selection Algorithm, J. Atmos. Ocean. Tech., 26, 1994–2014, 2009.

Oo, M. and Holz, R.: Improving the CALIOP aerosol optical depth using combined MODIS-CALIOP observations and CALIOP integrated attenuated total color ratio, J. Geophys. Res., 116, D14201, doi:10.1029/2010JD014894, 2011.

Osborne, S. R., Johnson, D. W., Wood, R., Bandy, B. J., Andreae, M. O., O'Dowd, C. D., Glantz, P., Noone, K. J., Gerbig, C., Rudolph, J., Bates, T. S., and Quinn, P.: Evolution of the aerosol, cloud and boundary-layer dynamic and thermodynamic characteristics during the 2nd Lagrangian experiment of ACE-2, Tellus B, 52, 375–400, 2000.

Powell, K. A., Hostetler, C. A., Liu, Z., Vaughan, M. A., Kuehn, R. E., Hunt, W. H., Lee, K.-P., Trepte, C. R., Rogers, R. R., Young, S. A., and Winker, D. M.: CALIPSO lidar calibration algorithms. Part I: Nighttime 532-nm parallel channel and 532-nm perpendicular channel, J. Atmos. Ocean. Tech., 26, 2015–2033, 2009.

Redemann, J., Zhang, Q., Schmid, B., Russell, P. B., Livingston, J. M., Jonsson, H., and Remer, L. A.: Assessment of MODIS-derived visible and near-IR aerosol optical properties and their spatial variability in the presence of mineral dust, Geophys. Res. Lett., 33, L18814, doi:10.1029/2006GL026626, 2006.

Reid, J. S., Kinney, J. E., Westphal, D. L., Holben, B. N., Welton, E. J., Tsay, S.-C., Eleuterio, D. P., Campbell, J. R., Christopher, S. A., Jonsson, H. H., Livingston, J. M., Maring, H. B., Meier, M., Pilewskie, P., Prospero, J., Reid, E. A., Remer, L. A., Russell, P. B., Savoie, D. L., Smirnov, A., and Tanre, D.: Analysis of measurements of Saharan dust by airborne and ground-based remote sensing methods during the Puerto Rico Dust Experiment (PRIDE), J. Geophys. Res., 108, 8586, doi:10.1029/2002JD002493, 2003.

Reid, J. S., Hyer, E. J., Prins, E. M., Westphal, D. L., Zhang, J., Wang, J., Christopher, S. A., Curtis, C. A., Schmidt, C. C., Eleuterio, D. P., Richardson, K. A., and Hoffman, J. P.: Global Monitoring and Forecasting of Biomass-Burning Smoke: Description of and Lessons from the Fire Locating and Modeling of Burning Emissions (FLAMBE) Program, IEEE J. Sel. Top. Appl., 2, 144–162, JSTARS-2009-00034, 2009.

Reid, J. S., Hyer, E. J., Johnson, R. S., Holben, B. N., Yokelson, R. J., Zhang, J., Campbell, J. R., Christopher, S. A., Di Girolamo, L., Giglio, L., Holz, R. E., Kearney, C., Miettinen, J., Reid, E. A., Turk, F. J., Wang, J., Xian, P., Zhao, G., Balasubramanian, R., Chew, B. N., Janai, S., Lagrosas, N., Lestari, P., Lin, N.-H., Mahmud, M., Anh, N. X., Norris, B., Oahn, N. T. K., Oo, M., Salinas, S. V., Welton, E. J., and Liew, S. C.: Observing the Southeast Asian aerosol system by remote sensing: a critical review for the Seven Southeast Asian Studies (7SEAS) program, Atmos. Res., online first: doi:10.1016/j.atmosres.2012.06.005, 2012.

Remer, L. A., Kaufman, Y. J., Tanre, D., Mattoo, S., Chu, D. A., Martins, J. V., Li, R.-R., Ichoku, C., Levy, R. C., Kleidman, R. G., Eck, T. F., Vermote, E., and Holben, B. N.: The MODIS aerosol algorithm, products, and validation, J. Atmos. Sci., 62, 947–973, 2005.

Rogers, R. R., Hostetler, C. A., Hair, J. W., Ferrare, R. A., Liu, Z., Obland, M. D., Harper, D. B., Cook, A. L., Powell, K. A., Vaughan, M. A., and Winker, D. M.: Assessment of the CALIPSO Lidar 532 nm attenuated backscatter calibration using the NASA LaRC airborne High Spectral Resolution Lidar, Atmos. Chem. Phys., 11, 1295–1311, doi:10.5194/acp-11-1295-2011, 2011.

Sassen, K. and Cho, B. S.: Subvisual-thin cirrus lidar dataset for satellite verification and climatological research, J. Appl. Meteor., 31, 1275–1285, 1992.

Schmid, B., Ferrare, R., Flynn, C. M., Elleman, R., Covert, D., Strawa, A., Welton, E. J., Turner, D. D., Jonsson, H., Redemann, J., Eilers, J., Ricci, K., Hallar, A. G., Clayton, M. B., Michalsky, J. J., Smirnov, A., Holben, B. N., and Barnard, J. C.: How well do state-of-the-art techniques measuring the vertical profile of tropospheric aerosol extinction compare?, J. Geophys. Res., 111, D05S07, doi:10.1029/2005JD005837, 2006.

Sekiyama, T. T., Tanaka, T. Y., Shimizu, A., and Miyoshi, T.: Data assimilation of CALIPSO aerosol observations, Atmos. Chem. Phys., 10, 39–49, doi:10.5194/acp-10-39-2010, 2010.

Shi, Y.: Development of data-assimilation-quality MODIS and MISR over water aerosol products, M. S. thesis, Department of Atmospheric Sciences, University of North Dakota, 74 pp., 2009.

Shi, Y., Zhang, J., Reid, J. S., Holben, B., Hyer, E. J., and Curtis, C.: An analysis of the collection 5 MODIS over-ocean aerosol optical depth product for its implication in aerosol assimilation, Atmos. Chem. Phys., 11, 557–565, doi:10.5194/acp-11-557-2011, 2011a.

Shi, Y., Zhang, J., Reid, J. S., Hyer, E. J., Eck, T. F., Holben, B. N., and Kahn, R. A.: A critical examination of spatial biases

between MODIS and MISR aerosol products – application for potential AERONET deployment, Atmos. Meas. Tech., 4, 2823–2836, doi:10.5194/amt-4-2823-2011, 2011b.

Stephens, G. L., Vane, D. G., Boain, R. J., Mace, G. G., Sassen, K., Wang, Z., Illingsworth, A. J., O'Connor, E. J., Rossow, W. B., Durden, S. L., Miller, S. D., Austin, R. T., Benedetti, A., and Mitrescu, C.: The Cloudsat mission and the A-Train, B. Am. Meteorol. Soc., 83, 1771–1790, doi:10.1175/BAMS-83-12-1771, 2002.

Tesche, M., Ansmann, A., Müller, D., Althausen, D., Mattis, I., Heese, B., Freudenthaler, V., Wiegner, M., Esselborn, M., Pisani, G., and Knippertz, P.: Vertical profiling of Saharah dust with Raman lidars and airborne HSRL in southern Morocco during SAMUN, Tellus B, 61, 144–164, 2009.

Tesche, M., Gross, S., Ansmann, A., Müller, D., Althausen, D., Freudenthaler, V., and Esselborn, M.: Profiling of Saharan dust and biomass-burning smoke with multiwavelength polarization Raman lidar at Cape Verde, Tellus B, 63, 649–676, 2011.

Uno, I., Yumimoto, K., Shimizu, A., Hara, Y., Sugimoto, N., Wang, Z., Liu, Z., and Winker, D. M.: 3D structure of Asian dust transport revealed by CALIPSO lidar and a 4DVAR dust model, Geophys. Res. Lett., 35, L06803, doi:10.1029/2007GL032329, 2008.

Uno, I., Eguchi, K., Yumimoto, K., Takemura, T., Shimizu, A., Uematsu, M., Liu, Z., Wang, Z., Hara, Y., and Sugimoto, N.: Asian dust transported one full circuit around the globe, Nat. Geosci., 2, 557–560, 2009.

Vaughan, M. A., Powell, K. A., Kuehn, R. E., Young, S. A., Winker, D. M., Hostetler, C. A., Hunt, W. H., Liu, Z., McGill, M. J., and Getzewich, B. J.: Fully automated detection of cloud and aerosol layers in the CALIPSO lidar measurements, J. Atmos. Ocean. Tech., 26, 2034–2050, 2009.

Wandinger, U., Tesche, M., Seifert, P., Ansmann, A., Müller, D., and Althausen, D.: Size matters: influence of multiple scattering on CALIPSO light-extinction profiling in desert dust, Geophys. Res. Lett., 37, L10801, doi:10.1029/2010GL042815, 2010.

Welton, E. J., Campbell, J. R., Spinhirne, J. D., and Scott, V. S.: Global monitoring of clouds and aerosols using a network of micro-pulse lidar systems, Proc. Int. Soc. Opt. Eng., 4153, 151–158, 2001.

Welton, E. J., Voss, K. J., Quinn, P. K., Flatau, P. J., Markowicz, K., Campbell, J. R., Spinhirne, J. D., Gordon, H. R., and Johnson, J. E.: Measurements of aerosol vertical profiles and optical properties during INDOEX 1999 using micro-pulse lidars, J. Geophys. Res., 107, 8019, doi:10.1029/2000JD000038, 2002.

Winker, D. M., Vaughan, M. A., Omar, A., Hu, Y., Powell, K. A., Liu, Z., Hunt, W. H., and Young, S. A.: Overview of the CALIPSO Mission and CALIOP Data Processing Algorithms, J. Atmos. Ocean. Tech., 26, 2310–2323, 2009.

Winker, D. M., Pelon, J., Coakley Jr., J. A., Ackerman, S. A., Charlson, R. J., Colarco, P. R., Flamant, P., Fu, Q., Hoff, R., Kittaka, C., Kubar, T. L., LeTreut, H., McCormick, M. P., Megie, G., Poole, L., Powell, K., Trepte, C., Vaughan, M. A., and Wielicki, B. A.: The CALIPSO mission: A global 3D view of aerosols and clouds, B. Am. Meteorol. Soc., 91, 1211–1229, 2010.

Winker, D. M., Tackett, J. L., Getzewich, B. J., Liu, Z., Vaughan, M. A., and Rogers, R. R.: The global 3-D distribution of tropospheric aerosols as characterized by CALIOP, Atmos. Chem. Phys. Discuss., in press, 2012.

Xian, P., Reid, J. S., Turk, J. F., Hyer, E. J., and Westphal, D. L.: Impact of modeled versus satellite measured tropical precipitation on regional smoke optical thickness in an aerosol transport model, Geophys. Res. Lett., 36, L16805, doi:10.1029/2009GL038823, 2009.

Young, S. A. and Vaughan, M. A.: The retrieval of profiles of particulate extinction from Cloud-Aerosol Lidar Infrared Pathfinder Satellite Observations (CALIPSO) data: algorithm description, J. Atmos. Ocean. Tech., 26, 1105–1119, 2009.

Yumimoto, K., Uno, I., Sugimoto, N., Shimizu, A., Liu, Z., and Winker, D. M.: Adjoint inversion modeling of Asian dust emission using lidar observations, Atmos. Chem. Phys., 8, 2869–2884, doi:10.5194/acp-8-2869-2008, 2008.

Zhang, J. and Reid, J. S.: MODIS aerosol product analysis for data assimilation: Assessment of level 2 aerosol optical thickness retrievals, J. Geophys. Res., 111, D22207, doi:10.1029/2005JD006898, 2006.

Zhang, J. and Reid, J. S.: An analysis of clear sky and contextual biases using an operational over ocean MODIS aerosol product, Geophys. Res. Lett., 36, L15824, doi:10.1029/2009GL038723, 2009.

Zhang, J. and Reid, J. S.: A decadal regional and global trend analysis of the aerosol optical depth using a data-assimilation grade over-water MODIS and Level 2 MISR aerosol products, Atmos. Chem. Phys., 10, 10949–10963, doi:10.5194/acp-10-10949-2010, 2010.

Zhang, J., Reid, J. S., and Holben B. N.: An analysis of potential cloud artifacts in MODIS over ocean aerosol optical thickness products, Geophys. Res. Lett., 32, L15803, doi:10.1029/2005GL023254, 2005.

Zhang, J., Reid, J. S., Westphal, D. L., Baker, N. L., and Hyer, E. J.: A system for operational aerosol optical depth data assimilation over global oceans, J. Geophys. Res., 113, D10208, doi:10.1029/2007JD009065, 2008.

Zhang, J., Campbell, J. R., Reid, J. S., Westphal, D. L., Baker, N. L., Campbell, W. F., and Hyer, E. J.: Evaluating the impact of assimilating CALIOP-derived aerosol extinction profiles on a global mass transport model, Geophys. Res. Lett., 38, L14801, doi:10.1029/2011GL047737, 2011.